

## JET-CLOUD INTERACTIONS IN COMPACT RADIO SOURCES

C. P. O’Dea,<sup>1</sup> W. H. De Vries,<sup>2</sup> A. M. Koekemoer,<sup>1</sup> S. A. Baum,<sup>1</sup> and J. Mack<sup>1</sup>

### RESUMEN

Presentamos espectros de rendija larga de *HST*/STIS de nebulas de emisión alineadas en 3 radiofuentes compactas de espectro empujado (inglés: Compact Steep Spectrum Sources, CSS). Encontramos desviaciones sistemáticas en los centroides de las líneas en ambos lados de la fuente de radio de 300–500 km s<sup>-1</sup> con valores similares en el ancho de líneas. No encontramos evidencia de curvas de rotación keplerianas. La asociación espacial entre las desviaciones en velocidad y los lóbulos en radio implica que las desviaciones de las líneas con respecto a la velocidad sistémica se deben probablemente a un flujo impulsado por la fuente de radio, sugiriendo que las fuentes de radio CSS son capaces de acelerar nubes ambientales hasta velocidades de 300–500 km s<sup>-1</sup>. Presentamos también las primeras imágenes de emisión Ly $\alpha$  en la fuente de radio con “cooling flow”—PKS 2322-123. Esta radiofuente de potencia mediana parece estar barriendo gas en el norte y estar desviada por una nube densa en el sur. Ly $\alpha$  es más brillante a la escala de la radiofuente indicando que la fuente de radio juega un papel en determinar el brillo de la emisión Ly $\alpha$  interior—ya sea por un aumento de la medida de emisión (“emission measure”) por compresión y/o por proveer parte de la energía para crear esa luminosidad. La emisión de Ly $\alpha$  se extiende hasta una escala de 25” de diámetro con una morfología difusa y filamentosa y con una razón Ly $\alpha$ /H $\alpha$  “estándar” (excepto en algunos de los filamentos interiores)—implicando que el polvo tiene un factor de llenado (“filling factor”) volumétrico bajo y está confinado principalmente a algunos pocos filamentos grumosos interiores. Por lo tanto, las fuentes CSS más poderosas y la fuente de baja potencia con “cooling flow” han tenido interacciones cualitativamente diferentes con su ambiente—aunque en ambos casos el gas emisor de líneas nos permite estudiar la interacción.

### ABSTRACT

We present *HST*/STIS long slit spectra of the aligned emission line nebulae in 3 powerful Compact Steep Spectrum (CSS) radio sources. We find systematic offsets in the line centroid on the two sides of the radio source of order 300–500 km s<sup>-1</sup> with similar values for the line widths. We do not find evidence for Keplerian rotation curves. The spatial association of the velocity offsets with the radio lobes implies that the line offsets from systemic are most likely due to outflow driven by the radio source, suggesting that CSS radio sources are capable of accelerating ambient clouds up to velocities of 300–500 km s<sup>-1</sup>. We also present the first *HST*/STIS images of Ly $\alpha$  emission in a “cooling flow” radio source—PKS 2322-123. The moderate power radio source appears to be sweeping up gas in the north and to be deflected by a dense cloud in the south. The Ly $\alpha$  is brightest on the scale of the radio source which suggests that the radio source plays a role in determining the brightness of the inner Ly $\alpha$  emission—either by enhancing the emission measure through compression and/or by providing some of the energy to power the luminosity. The Ly $\alpha$  extends out to scales of 25” diameter with a diffuse, filamentary morphology and with a “standard” Ly $\alpha$ /H $\alpha$  ratio (except in some of the inner filaments)—implying that the dust has a low volume filling factor and is confined mainly to a few clumpy inner filaments. Thus, the more powerful CSS sources and the lower power “cooling flow” source have had qualitatively different interactions with their environment—although in both cases the emission line gas allows us to probe that interaction.

*Key Words:* GALAXIES: ACTIVE — GALAXIES: ISM — GALAXIES: JETS — GALAXIES: KINEMATICS AND DYNAMICS — ISM: JETS AND OUTFLOWS

#### 1. WHAT ARE CSS SOURCES?

Recent work has identified the GHz Peaked Spectrum (GPS) and Compact Steep Spectrum (CSS) radio sources as the most likely candidates for the

progenitors of the large scale powerful classical double (3CR FR2) sources (e.g., O’Dea, Baum, & Stanghellini 1991; Fanti et al. 1990; Fanti et al. 1995; Readhead et al. 1996a,b; O’Dea & Baum 1997, for a review see O’Dea 1998). The GPS and CSS sources are powerful but compact radio sources whose spectra are generally simple and convex with peaks near

<sup>1</sup>Space Telescope Science Institute, Baltimore, USA.

<sup>2</sup>IGPP, Lawrence Livermore National Laboratory, USA.

1 GHz and 100 MHz respectively. The GPS sources are entirely contained within the extent of the narrow line region ( $\lesssim 1$  kpc) while the CSS sources are contained entirely within the host galaxy ( $\lesssim 15$  kpc).

Current models for the evolution of powerful radio galaxies suggest that these sources propagate from the  $\sim 10$  pc to Mpc scales at roughly constant velocity through an ambient medium which declines in density as  $\rho(R) \propto R^{-2}$  while the sources decline in radio luminosity as  $L_{\text{rad}} \propto R^{-0.5}$  (Fanti et al. 1995; Begelman 1996; Readhead et al. 1996b; De Young 1997; Kaiser & Alexander 1997; Kaiser, Dennett-Thorpe, & Alexander 1997). The observed number densities of powerful radio sources as a function of linear size (from tens of parsecs to hundreds of kpc) are consistent with such a scenario (O’Dea & Baum 1997; O’Dea 1998). However, the situation must be more complicated than this simple picture. (1) The GPS and CSS sources must interact with the host galaxy as they propagate through it. The discovery of emission line gas aligned with and presumably co-spatial with the CSS radio sources indicates that the radio source is strongly interacting with the ambient gas (De Vries et al. 1997, 1999; Axon et al. 2000). Interestingly, for four of the six sources for which deep [O III] imaging was obtained by Axon et al. fainter aligned line emission extends well beyond the radio source. Therefore, while shock ionization (Bicknell, Dopita, & O’Dea 1997) is probably the dominant excitation process in the innermost regions of line emission, photo-ionization may be important in regions beyond the radio source. (2) The GPS sources are observed to have proper motions several times higher (Conway 1998, private communication) than the estimated advance speeds of large scale classical doubles (Alexander & Leahy 1987). This would require the GPS sources to decelerate as they propagate through the host galaxy and would require the radio sources to dim faster than the simple models predict. It may be that the deceleration takes place via interaction with the ambient gas that is probed by our observations.

It is clear that the statistical results based on number counts of powerful radio sources are not sufficient by themselves to constrain the models for radio source evolution. We need a more direct probe of the radio source propagation through the host galaxy. Fortunately, the aligned emission line gas in CSS sources recently discovered by De Vries et al. (1997, 1999) and Axon et al. (2000) provides such a powerful diagnostic probe. The close alignment and similar spatial extents of the radio and emission line plasma suggest the existence of a close cou-

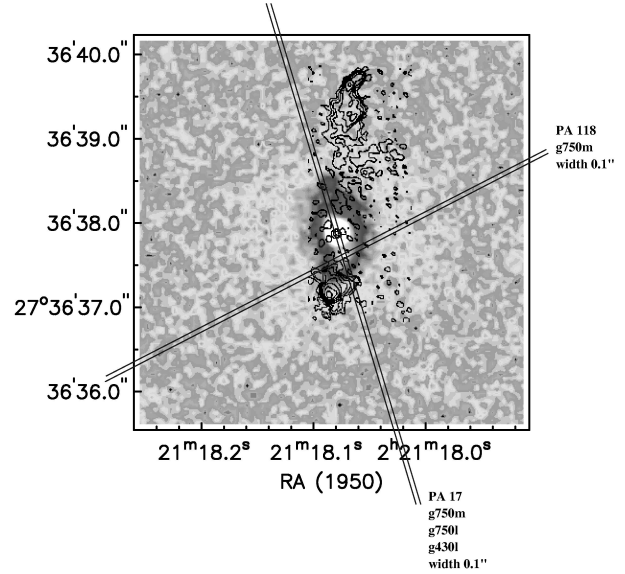


Fig. 1. STIS slit orientations are shown on a gray-scale plot of the *HST*/WFPC2 F702W image of 3C67 with contours of the radio image. NOTE: THIS FIGURE IS AVAILABLE IN COLOR IN THE ELECTRONIC VERSION OF THIS ARTICLE, OBTAINABLE FROM <http://www.astroscu.unam.mx/~rmaa/>.

pling between the thermal gas and the radio sources. The broad and highly structured spatially integrated [O III]  $\lambda 5007$  line widths observed by Gelderman & Whittle (1994, hereafter GW94) strongly suggest that the radio source is dominating the emission line kinematics.

## 2. THE ALIGNMENT EFFECT IN CSS SOURCES

Broad and narrow band *HST* imaging of CSS radio sources (De Vries et al. 1997, 1999; Axon et al. 2000) have shown the following. CSS radio galaxies at all redshifts exhibit emission line gas which is strongly aligned with the radio source. The alignment is much stronger than seen in low redshift large-scale radio galaxies and is similar to that seen in high- $z$  ( $\gtrsim 0.6$ ) radio galaxies. In most cases the emission line gas lies interior to the radio hot spots. However, in a few cases fainter emission is found beyond the radio source.

The close association between the gas and the radio source suggests that the radio source interacts strongly with the ambient medium as it propagates through the ISM. The fainter gas outside the radio source is possibly photoionized, while bright gas interior to the hotspots has been shocked by the radio source. Cooling time arguments applied to the gap between the radio hot spots and the onset of bright emission line gas are consistent with lobe ex-

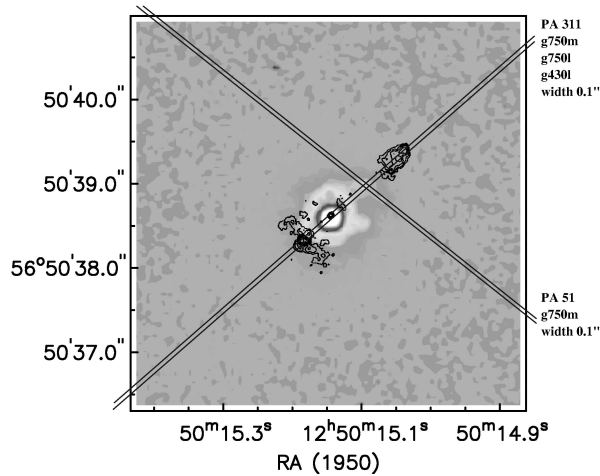


Fig. 2. Same as Fig. 1 but for 3C277.1. NOTE: THIS FIGURE IS AVAILABLE IN COLOR IN THE ELECTRONIC VERSION OF THIS ARTICLE, OBTAINABLE FROM <http://www.astroscu.unam.mx/~rmaa/>.

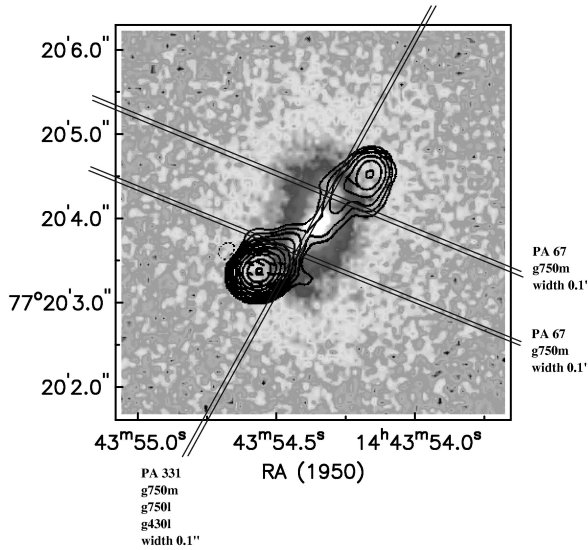


Fig. 3. Same as Fig. 1 but for 3C303.1. NOTE: THIS FIGURE IS AVAILABLE IN COLOR IN THE ELECTRONIC VERSION OF THIS ARTICLE, OBTAINABLE FROM <http://www.astroscu.unam.mx/~rmaa/>.

pansion velocities  $\gtrsim 1000 \text{ km s}^{-1}$  for ambient densities of  $n \sim 1 \text{ cm}^{-3}$ . (3C303.1 is consistent with  $V_{\text{lobe}} \gtrsim 6000 \text{ km s}^{-1}$ .)

### 3. THE STIS LONG SLIT SPECTROSCOPIC OBSERVATIONS

The goal of the STIS observations is to study the kinematics and ionization of gas aligned with the radio source in 3 CSS sources: 3C67 ( $z = 0.310$ ),

3C277.1 ( $z = 0.321$ ), 3C303.1 ( $z = 0.267$ ).<sup>3</sup> In this paper we report on our preliminary results on the kinematics of the gas in these three sources.

The main characteristics of the observations are the following. We obtained STIS long slit spectra through G750M centered on [O III]  $\lambda 5007$ , with a resolution of  $0.56 \text{ \AA}/\text{pixel}$  and slit width  $0''.1$ . We integrated for one orbit on each slit ( $\sim 2500\text{--}3000 \text{ sec}$ ) with the orientation taken parallel and perpendicular to the radio source axis. The  $\perp$  slit was centered on the brightest feature of the nebula. We obtained  $\perp$  slits on both the N and S lobe in 3C303.1 and only one lobe in the other two sources (see Figures 1, 2, 3).

## 4. RESULTS ON INDIVIDUAL SOURCES

### 4.1. 3C67

**Parallel to the radio axis** Illustrated in Figure 4(a) The N lobe is near the systemic velocity, while the S lobe is blue shifted by  $\sim 300 \text{ km s}^{-1}$ . There are no systematic gradients along the individual lobes. The line FWHM are  $\sim 200 \text{ km s}^{-1}$ .

**Perpendicular to the radio axis** Illustrated in Figure 4(b). The line width is  $\sim 300 \text{ km s}^{-1}$ . There is no velocity gradient across the bright knot in the lobe.

### 4.2. 3C277.1

**Parallel to the radio axis** Illustrated in Figure 4(c). The S lobe is near the systemic velocity, while the N lobe is redshifted by  $\sim 300 \text{ km s}^{-1}$ . There are no systematic gradients along the individual lobes. The line FWHM  $\sim 200 \text{ km s}^{-1}$ .

**Perpendicular to the radio axis** Illustrated in Figure 4(d). The line FWHM  $\sim 300 \text{ km s}^{-1}$ . The velocity is slightly higher in the center of the lobe than the edges by  $\sim 150 \text{ km s}^{-1}$ .

### 4.3. 3C303.1

**Parallel to the radio axis** Illustrated in Figure 5(a). There is a complex velocity field showing several components (split lines?) and/or broader lines with FWHM  $\sim 500 \text{ km s}^{-1}$ . There is a velocity shift from systemic of  $\sim 500 \text{ km s}^{-1}$  on the S lobe and  $\sim 250 \text{ km s}^{-1}$  on the N lobe.

**Perpendicular to the radio axis** Illustrated in Figures 5(b,c). Both lobes show evidence for multiple components (split lines?) and/or broad line widths  $\sim 750 \text{ km s}^{-1}$  (However, this is uncertain due to the low S/N in the lines).

<sup>3</sup>We adopt a Hubble constant of  $H_0 = 75 \text{ km s}^{-1} \text{ Mpc}^{-1}$  and a deceleration parameter of  $q_0 = 0.0$ .

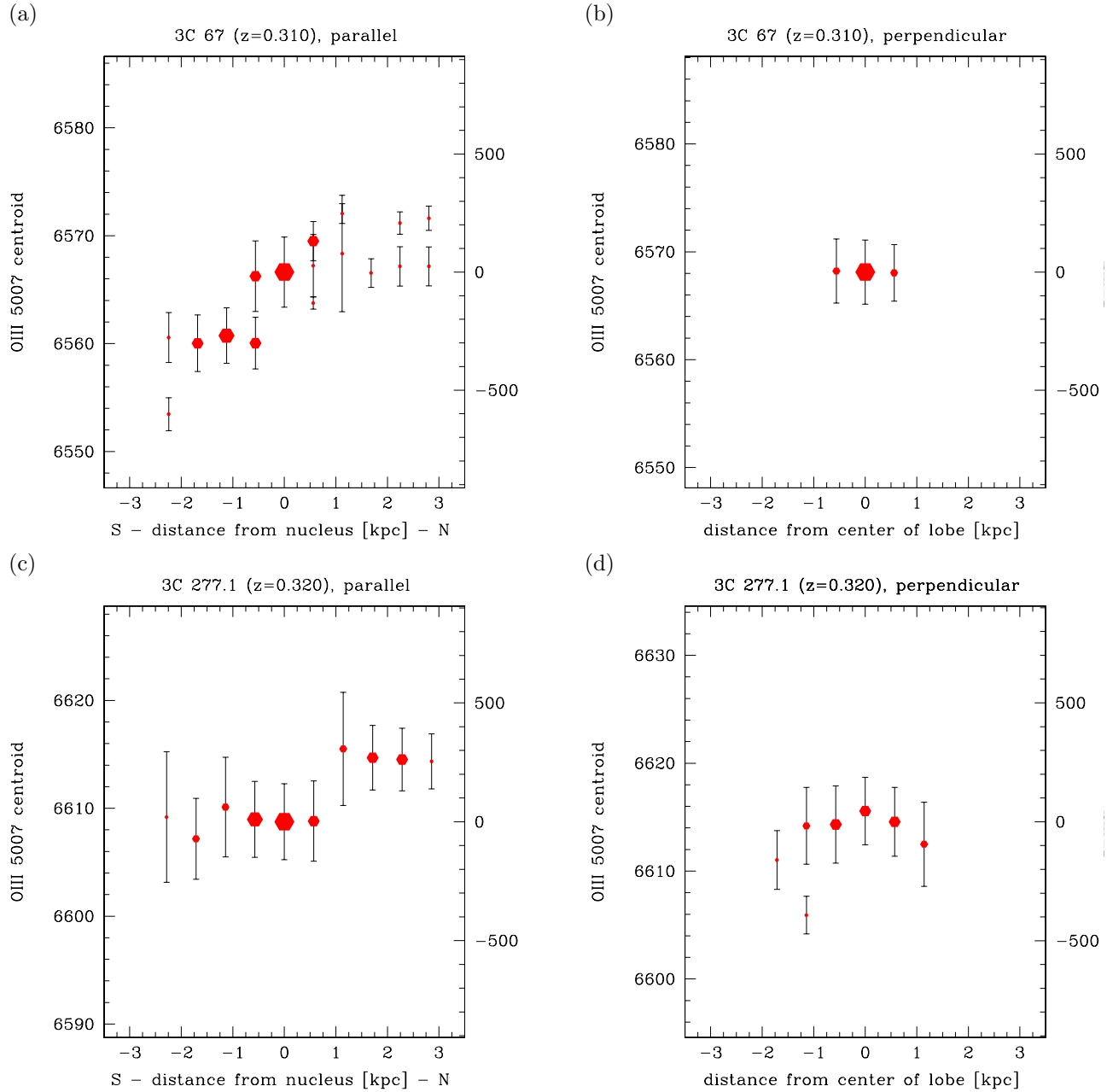


Fig. 4. Plot of emission line kinematic properties as a function of distance along the slit. The size of the symbol is proportional to the line flux. The bars denote the line FWHM, not the errors on the line centroid which are quite small. (a) 3C67, slit parallel to the radio source axis; (b) 3C67 Southern lobe, slit perpendicular to the radio source axis; (c) 3C277.1, slit parallel to the radio source axis; (d) 3C277.1 Northern lobe, slit perpendicular to the radio source axis.

5. IMPLICATIONS

The kinematics are inconsistent with illumination of a *quiescent* ISM by an active nucleus. We see systematic offsets in velocity of the gas on the two sides of the radio source. There is no evidence for Keplerian rotation in the gas. The velocity offsets must be either infall or outflow. The association of the gas

with the radio source supports the hypothesis that the gas bulk motions are outflow driven by the jets.

The slit across the lobe of 3C277.1 shows higher blue shifted velocities (by  $\sim 150 \text{ km s}^{-1}$ ) in the center than the edges of the lobe. This is qualitatively similar to that expected from an expanding bow shock. However, in that case we would also ex-

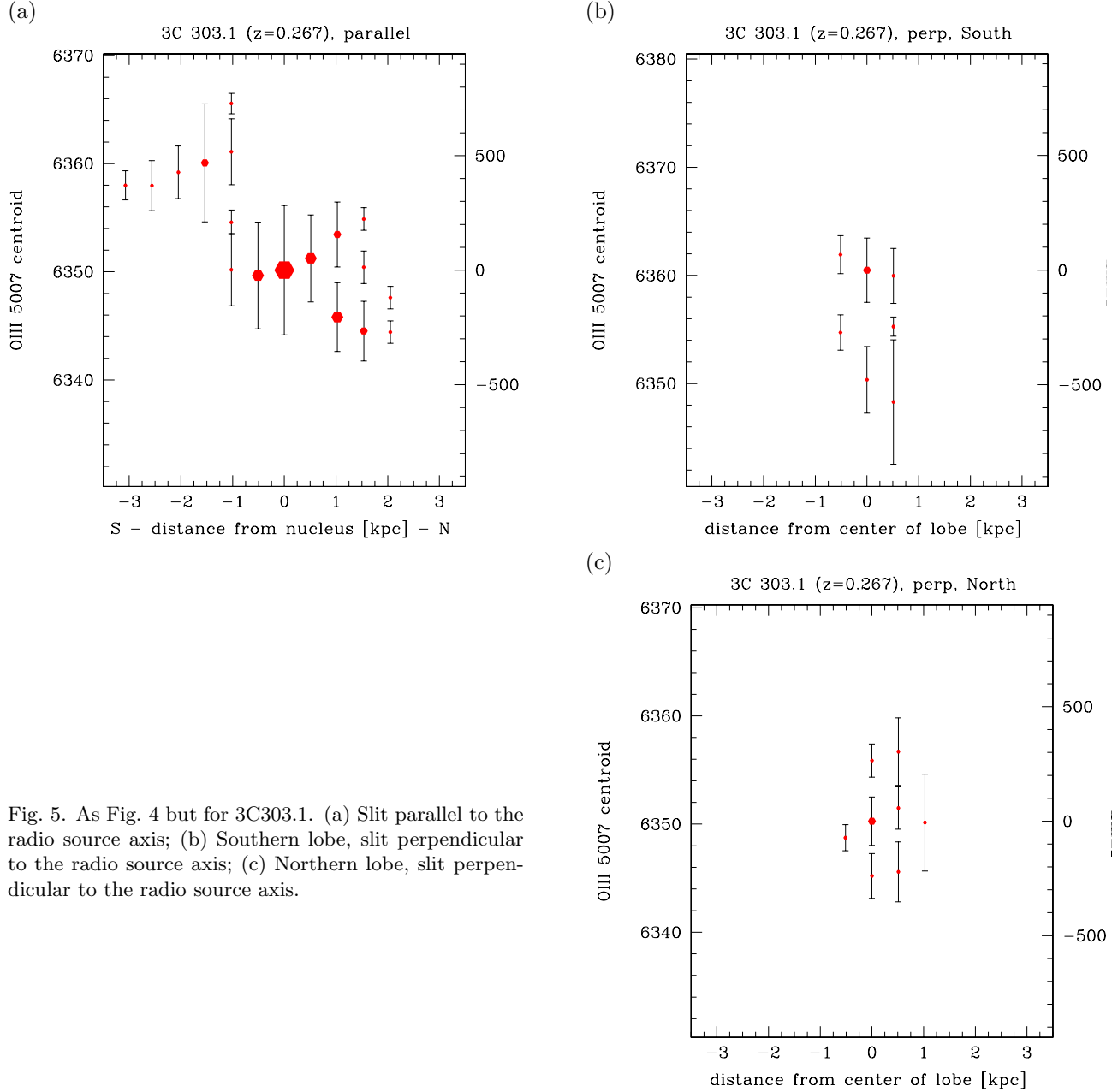


Fig. 5. As Fig. 4 but for 3C303.1. (a) Slit parallel to the radio source axis; (b) Southern lobe, slit perpendicular to the radio source axis; (c) Northern lobe, slit perpendicular to the radio source axis.

pect to see line splitting unless (1) the line splitting is less than the line FWHM or (2) if there is asymmetry in the emissivity causing the gas on one side of the lobe to be fainter than on the other.

In 3C303.1, we do see evidence for either very broad lines or multiple components (possibly split lines) in both radio lobes. In the case of split lines, the data are consistent with a difference in the line centroids of  $\sim 500 \text{ km s}^{-1}$ .

Thus, CSS radio sources are capable of accelerating clouds up to velocities of  $\sim 300\text{--}500 \text{ km s}^{-1}$ . However, this is still factors of a few-ten smaller than

the expected forward propagation speed of the lobes. This could be due to the the clouds not being accelerated to the initial shock velocity (e.g., Klein, McKee, & Colella 1994; Villar-Martín et al. 1999). In addition, numerical simulations of powerful jets have shown that the lateral expansion velocity of both the bow shock and the cocoon decreases quickly behind the jet head (Carvalho & O’Dea, in preparation). Thus, over most of the lifetime of the source, the ambient clouds are embedded in a medium which is moving roughly at the sound speed rather than at the much higher propagation speed of the radio source.

Abell 2597 (10"x10")

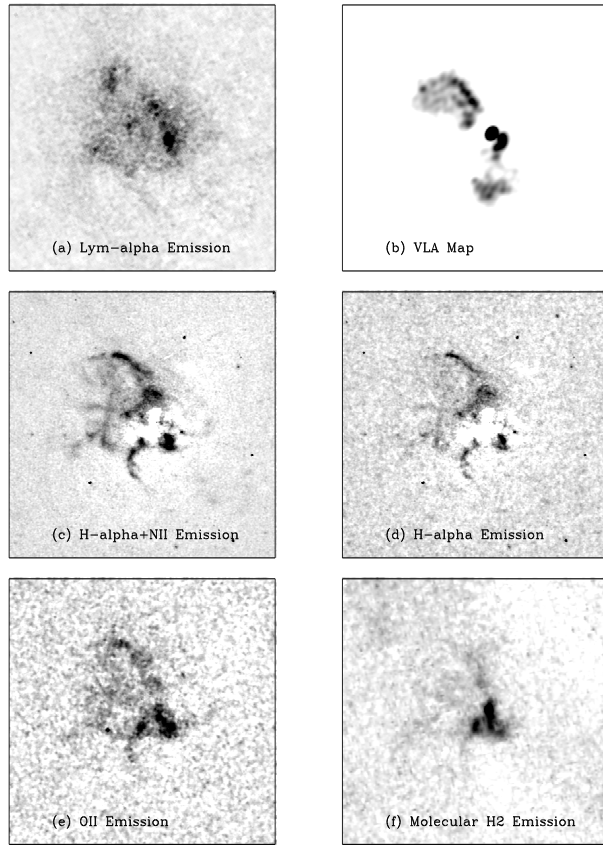


Fig. 6. PKS 2322–123. Montage of the VLA radio image (Sarazin et al. 1995) and *HST* emission line images. The  $H_2$  image is from Donahue et al. (2000). As shown by Koekemoer et al. (1999) the radio source appears to be interacting with the ambient medium.

## 6. JET-CLOUD INTERACTIONS IN THE 'COOLING-FLOW' RADIO SOURCE PKS 2322–123

PKS 2322–123 ( $z = 0.0821$ ) is associated with the central dominant galaxy in the rich cluster A2597. The X-ray emission has been characterized as having a cooling flow with a mass accretion rate  $\sim 150 M_{\odot} \text{ yr}^{-1}$  (e.g., Sarazin & McNamara 1997). The source sits within a very extended and luminous optical emission line nebula (Heckman et al. 1989; Crawford & Fabian 1992), which is rich in atomic hydrogen (O’Dea, Baum, & Gallimore 1994).

The source is lower power than the 3 CSS sources discussed above and possibly sits in a denser, more gas-rich environment. Here we probe the nature of the interaction with the ambient medium using WFPC2 imaging (Koekemoer et al. 1999), NICMOS  $H_2$  imaging (Donahue et al. 2000) and new STIS Far-

UV MAMA  $\text{Ly}\alpha$  imaging (Baum et al. 2001). These are the first *HST*  $\text{Ly}\alpha$  images of a cooling flow cluster.

### 6.1. *HST* Results

We observed PKS 2322–123 with the STIS Far-UV MAMA through the F25SRF2 (on-band  $\text{Ly}\alpha$ ) and F25QTZ (off-band Far-UV continuum) filters for 1000s each. A montage of the radio image and *HST* emission line images is shown in Figure 6. As shown by Koekemoer et al. (1999) the radio source is interacting strongly with its environment—the northern lobe appears to have swept up a shell of gas creating bright emission line arcs on the edge of the radio lobe—while the southern jet appears to be deflected by a collision with a dense gas cloud. Both the filaments and the dense cloud emit in  $\text{Ly}\alpha$ ,  $H\alpha$ , and  $H_2$  implying that the gas contains a range of temperatures and ionization states ranging from molecular to atomic to ionized and that the gas has experienced shocks (possibly induced by the radio source).

We note that both  $H\alpha$  and  $\text{Ly}\alpha$  are weak in the very dusty filaments near the nucleus—where  $H_2$  is enhanced. Our  $\text{Ly}\alpha/H\alpha$  ratio image (not shown here) reveals that the on the scale of a few arcseconds the more diffuse emission and part of the bright filaments have the “standard” ratio of 10 indicating an absence of dust, while some parts of the bright filaments have lower ratios implying that here  $\text{Ly}\alpha$  is suppressed due to the presence of dust. This implies that the dust has a low volume filling factor and is confined mainly to the highly clumped regions in the center and in parts of the  $H\alpha$ -bright emission line filaments.

A larger-scale view of the  $\text{Ly}\alpha$  is shown in Figure 7. It is clear that the  $\text{Ly}\alpha$  is brightest in the central region on the scale of the radio source. This suggests that the radio source plays a role in determining the brightness of the inner  $\text{Ly}\alpha$  emission—either by enhancing the emission measure through compression and/or by providing some of the energy to power the luminosity. In addition, the  $\text{Ly}\alpha$  extends out on scales of  $25''$  diameter (coincident with the extended  $H\alpha$  nebula—Heckman et al. 1989) with a diffuse, filamentary morphology.

Thus, PKS 2322–123 is a lower luminosity source which has had qualitatively different interactions with the ambient gas than the more luminous/powerful CSS sources. The *HST* observations provide a wealth of diagnostics for probing the interaction between the radio source and ambient medium.

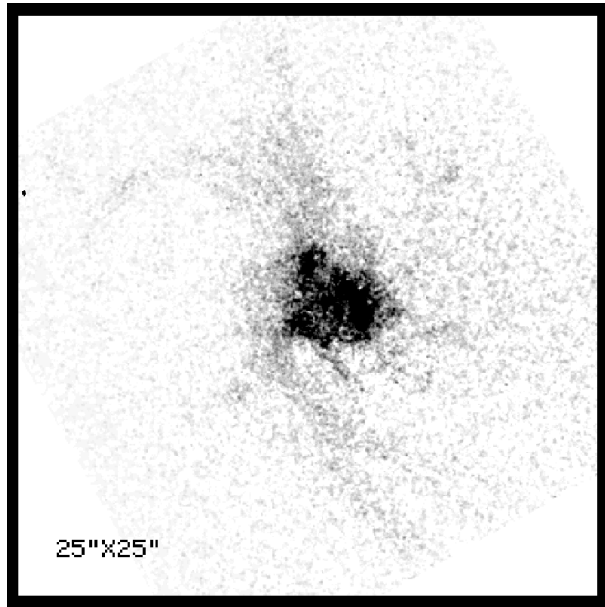


Fig. 7. PKS 2322–123. STIS FUV-MAMA image of the Ly $\alpha$  line on the 25'' scale.

We are very grateful to our collaborators D. Axon, P. Barthel, A. Capetti, R. Fanti, R. Gelderman, A. Laor, R. Morganti, and C. Tadhunter. This work was based on observations made with the NASA/ESA *Hubble Space Telescope*. STScI is operated by the Association of Universities for Research in Astronomy, Inc. under the NASA contract NAS 5-26555. This work was partially supported by STScI grants GO-08104.01-97A and GO-08107.01-97A.

#### REFERENCES

- Alexander, P., & Leahy, J. P. 1987, *MNRAS*, 225, 1
- Axon, D. J., Capetti, A., Fanti, R., Morganti, R., Robinson, A., & Spencer, R. 2000, *AJ*, 120, 2284
- Baum, S. A., O'Dea, C. P., Koekemoer, A. M., Mack, J., & Laor, A. 2001, in *ASP Conf. Ser.* 249, *The Central Kiloparsec of Starbursts and AGN: The La Palma Connection*, eds. J. H. Knapen, J. E. Beckman, I. Shlosman, & T. J. Mahoney (San Francisco: ASP), 294
- Begelman, M. C. 1996, in *Cygnus A—Study of a Radio Galaxy*, eds. C. Carilli and D. Harris, (Cambridge: Cambridge University Press), 209
- Bicknell, G., Dopita, M. A., & O'Dea, C. P. 1997, *ApJ*, 485, 112
- Crawford, C. S., & Fabian, A. C. 1992, *MNRAS*, 259, 265
- De Vries, W., O'Dea, C. P., Baum, S. A., et al. 1997, *ApJS*, 110, 191
- De Vries, W. H., O'Dea, C. P., Baum, S. A., & Barthel, P. D. 1999, *ApJ*, 526, 27
- De Young, D. S. 1997, *ApJ*, 490, L55
- Donahue, M., Mack, J., Voit, G. M., Sparks, W., Elston, R., & Maloney, P. R. 2000, *ApJ*, 545, 670
- Fanti, C., Fanti, R., Dallacasa, D., Schilizzi, R. T., Spencer, R. E., & Stanghellini, C. 1995, *A&A*, 302, 317
- Fanti, R., Fanti, C., Schilizzi, R. T., Spencer, R. E., Rendon, N., Parma, P., van Breugel, W. J. M., & Venturi, T. 1990, *A&A*, 231, 333
- Gelderman, R., & Whittle, M. 1994, *ApJS*, 91, 491 (GW94)
- Heckman, T. M., Baum, S. A., van Breugel, W. J. M., & McCarthy, P. 1989, *ApJ*, 338, 48
- Kaiser, C. R., & Alexander, P. 1997, *MNRAS*, 286, 215
- Kaiser, C. R., Dennett-Thorpe, J., & Alexander, P. 1997, *MNRAS*, 292, 723
- Klein, R., McKee, C., & Colella, P. 1994, *ApJ*, 420, 213
- Koekemoer, A. M., O'Dea, C. P., Sarazin, C. L., McNamara, B. R., Donahue, M., Voit, G. M., Baum, S. A., & Gallimore, J. F. 1999, *ApJ*, 525, 621
- O'Dea, C. P. 1998, *PASP*, 110, 493
- O'Dea, C. P., & Baum, S. A. 1997, *AJ*, 113, 148
- O'Dea, C. P., Baum, S. A., & Gallimore, J. F. 1994, 436, 669
- O'Dea, C. P., Baum, S. A., & Stanghellini, C. 1991, *ApJ*, 380, 66
- Readhead, A. C. S., et al. 1996a, *ApJ*, 460, 612
- Readhead, A. C. S., Taylor, G. B., Xu, W., Pearson, T. J., Wilkinson, P. N., & Polatidis, A. G. 1996b, *ApJ*, 460, 634
- Sarazin, C. L., Burns, J. O., Roettiger, K., & McNamara, B. R. 1995, *ApJ*, 447, 559
- Sarazin, C. L., & McNamara, B. R. 1997, *ApJ*, 480, 203
- Villar-Martín, M., Tadhunter, C., Morganti, R., Axon, D., & Koekemoer, A. 1999, *MNRAS*, 307, 34

S. A. Baum, A. M. Koekemoer, J. Mack, and C. P. O'Dea: Space Telescope Science Institute, 3700 San Martin Dr., Baltimore, MD 21218, USA (sbaum,koekemoe,mack,odea@stsci.edu).

W. H. De Vries: Institute of Geophysics and Planetary Physics, Lawrence Livermore National Laboratory, Livermore, CA, 94550, USA (devries@llnl.gov).